Theoretical studies of strongly correlated rare-earth intermetallics RIn3 and RSn3 (R= Sm, Eu, and Gd)

M. Shafiq, Iftikhar Ahmad, and S. Jalali Asadabadi

Citation: Journal of Applied Physics **116**, 103905 (2014); doi: 10.1063/1.4894833
View online: http://dx.doi.org/10.1063/1.4894833
View Table of Contents: http://scitation.aip.org/content/aip/journal/jap/116/10?ver=pdfcov
Published by the AIP Publishing

JOURNAL OF APPLIED PHYSICS **116**, 103905 (2014)

Theoretical studies of strongly correlated rare-earth intermetallics RIn_3 and RSn_3 (R = Sm, Eu, and Gd)

M. Shafiq,[1,2] Iftikhar Ahmad,[1,2,a)] and S. Jalali Asadabadi[3]
[1]*Center for Computational Materials Science, University of Malakand, Chakdara, Pakistan*
[2]*Department of Physics, University of Malakand, Chakdara, Pakistan*
[3]*Department of Physics, Faculty of Science, University of Isfahan, Hezar Gerib Avenue, Isfahan 81744, Iran*

(Received 17 July 2014; accepted 26 August 2014; published online 9 September 2014)

In this paper, the structural, elastic, and electronic properties of RIn_3 and RSn_3 (R = Sm, Eu, Gd) compounds have been investigated using the full potential linearized augmented plane wave plus local orbital method within the density functional theory. The structural properties are investigated using the LDA, GGA, and the band correlated LDA+U and GGA+U schemes. The lattice parameters are in good agreement with the available experimental results and the divalent state of Eu is also verified. The spin-orbit coupling is included in order to predict the correct electronic properties and splitting of 4f states of the rare earth elements is also incorporated. We calculated Bulk modulus, shear modulus, Young's modulus, anisotropic ratio, Kleinman parameters, Poisson's ratio, Lame's co-efficient, sound velocities for shear and longitudinal waves, and Debye temperature. We also predict the Cauchy pressure and B/G ratio in order to explore the ductile and brittle behaviors of these compounds. © *2014 AIP Publishing LLC*.
[http://dx.doi.org/10.1063/1.4894833]

I. INTRODUCTION

The rare earth elements and, in particular, lanthanide series are well known due to their incomplete 4f shell. The unpaired electron in the 4f shell mainly determines the physical properties of the rare-earth elements and compounds.[1,2] The rare-earth intermetallic compounds have been an attractive area under discussion to the researchers due to their unique variety of interesting properties such as high melting point, high temperature ductility, high temperature mechanical properties, and good electrical and magnetic properties, which make them potential candidates for automobile, aviation, and aerospace application. In addition, high strength and stiffness, low specific weight corrosion resistance make rare-earth intermetallic better than other metals and made them useful for developing commercial aircraft turbines.[3] Due to absence of d electrons near the Fermi level, almost 90% of intermetallic compounds show ductile nature.[4]

Intermetallic compounds RSn_3 and RIn_3 (R = rare earth) show many interesting properties due to their incomplete 4f shell such as the presence of various magnetic structures, magnetic to non magnetic transition, valence fluctuations, and magnetic moment formation.[5,6] RSn_3 intermetallic compounds are used as best alternative of lead and improve the performance of lead-free solders.[7]

Rare earth (RE) intermetallic compounds RIn_3 and RSn_3 (R = Sm, Eu, Gd) have cubic $AuCu_3$-type crystal structure space group Pm-3m (No. 221) exhibit a verity of phenomena.[8,9] In the $AuCu_3$ structure, the rare earth atoms (R) are located in 1a (0, 0, 0) position. The non-magnetic elements In or Sn occupy 3c (0, ½, ½) position[9] Most of RIn_3 and RSn_3 compound order anti-ferromagnetically (AFM) at low temperature below 45 K.[10–12]

The stability of the RIn_3 and RSn_3 phase decreases along the light rare earths from La to Gd.[13] From magnetic measurement and lattice constant value, the rare earth exhibit the characteristic lanthanide contraction, with the exception of those of the Eu and Yb compounds in which the rare earth ions are divalent.[14]

In RIn_3 series, $SmIn_3$, $EuIn_3$, and $GdIn_3$ compounds indicates AFM transition with Neel temperature $T_N = 16$ K, 10 K, and 42 K, respectively.[15–17] For RSn_3 series, the compounds $SmSn_3$, $EuSn_3$, and $GdSn_3$ exhibits AFM transition at temperature $T_N = 12$ K, 36.5 K, and 16.5 K, respectively.[18] Magnetic properties and the lattice parameters for of the lanthanide RIn3 series were reported by Buschow *et al.*[12] from magnetic susceptibilities measurements they conclude that at low temperature most of the lanthnides RIn_3 series compounds are AFM ordering. Sanchez *et al.*[18] calculated the electronic and magnetic properties of RSn_3, compounds (R = La, Ce, Pr, Nd, Sm, Eu, Gd, Yb) using Mossbauer resonance. They found that Eu and Gd compounds point to complex magnetic structures. The Fermi surface properties of RIn_3 and RSn_3 were determined by Onuki and Settai.[19] The structural properties such as lattice parameter and bulk modulus of RSn_3 (R = Sm, Eu, and Gd) have been calculated by Asadabadi *et al.*[20] using local density approximation (LDA), generalized gradient approximation (GGA), and GGA + spin polarized approximations under the framework of WIEN97 code. Endoh *et al.*[21] experimentally calculated the elastic constants and the crystalline electric field effect on the elastic constants of the series of compounds SmX_3 (X = Pd, In, Sn, Tl, Pb) by means of the ultrasonic measurements. Valency of rare earth in RIn_3 and RSn_3 and the influence of valency on the electric field gradients (EFG) have been interpreted by Asadabadi *et al.*[8] using density functional theory (DFT).

a)Author to whom correspondence should be addressed. Electronic mail addresses: ahma5532@gmail.com and dr.iftikhar@uom.edu.pk Tele.: (092)332-906-7866

The elastic constants find out the response of the compounds to the external forces. The elastic constants determine the strength, brittleness/ductility, and hardness of materials. It also provides information about bonding character, anisotropy, and structural stability.[22]

In this paper, we report the structural, electronic, elastic, and mechanical properties of rare earth RIn_3 and RSn_3 (R = Sm, Eu, Gd) compounds using full potential linearized augmented plane wave plus local orbitals (FP-LAPW+lo) method under the frame work of DFT. The present study is important because it reports for the first time elastic, mechanical, and thermal properties of these compounds by *ab-initio* calculation.

II. METHOD OF CALCULATIONS

In the present study, calculations have been performed by using DFT implemented in the WIEN2k code[23] and employing the FP-LAPW+lo method.[24] The exchange correlation effects was calculate within the LDA[25] and GGA[26] with spin polarization. It is well known that Sn, Eu, and Gd are strongly correlated systems with localized 4f electrons therefore to obtain the exact nature of electronic structure LDA+U and GGA+U are used. The GGA+U method based on the Hubbard model and treated strongly correlated systems with an orbital dependence potential of Coulomb and exchange interaction.[27] Spin-orbit coupling (SOC) is included as relativistic effects. The radii of muffin-tin sphere have been chosen as 2.50 a. u. for the rare-earth elements as well as for Sn and In. To achieve convergence, the basis set expands in term of plane waves up to $R_{MT}\,K_{max} = 7$, where R_{MT} is the smallest atomic radius in a unit cell and K_{max} is the magnitude of the maximum value of k-vector in the plane waves expansion. For the valence wave function inside a muffin-tin spheres, the maximum value of angular momentum $l_{MAX} = 10$ were taken. In the interstitial region, the charge density were Fourier expanded up to $G_{max} = 12$. High accuracy is required to calculate elastic properties, therefore a dense k mesh of 165 k-points are taken in the irreducible wedge of the Brillouin zone with grid size $18 \times 18 \times 18$ using the Monkhorst and Pack mesh.[28]

In this work, we use Cubic-elastic software available at WIEN2k website[29] within GGA[26] with spin polarization to calculate the elastic properties. The calculations for elastic constants C_{11}, C_{12}, and C_{44} are also performed without spin polarization and the results are compared with the spin polarized results. The details about Cubic-elastic software are available in Ref. 30. We use energy approach[31] implemented in WIEN2k code.[23] Using Voigt notations by replacing and taking into account the additional symmetry imposed by the crystal symmetry, the number of elastic constants decreases. In particular for a cubic lattice, only three independent elastic constants C_{11}, C_{12}, and C_{44} are remains.

III. STRUCTURAL PROPERTIES

The structural properties of RIn_3 and RSn_3 (Sm, Eu, and Gd) are calculated by finding the total energy of the unit cell for each compound with respect to volume using Birch–Murnaghan equation of state.[32] Lattice constants and bulk moduli are obtained by LDA, GGA, LDA+U, and GGA+U potentials. The theoretically calculated results along with the available experimental data are tabulated in Table I. The table shows that GGA lattice constants of $SmSn_3$ and $GdSn_3$ are in closer agreement to experiment than GGA+U lattice constants of $SmSn_3$ and $GdSn_3$, whereas GGA+U lattice constant of $EuSn_3$ is closer to experiment than GGA lattice constants of $EuSn_3$. This confirms that $SmSn_3$ and $GdSn_3$ behave as itinerant compounds, whereas $EuSn_3$ behaves as localized compound. This in turn verifies that $EuSn_3$ is a divalent system, while $SmSn_3$ and $GdSn_3$ are trivalent. The same is true for the RIn_3 cases where R = Sm, Eu, and Gd. Table I also shows as we move from Sm to Gd that the lattice constants are contracted, which attributed to the lanthanide contraction, i.e., the decrease in atomic radius along the lanthanide series from left to right due to poor shielding effect of the 4f electrons with exception for Eu and Yb which display divalency in 4f series ($EuIn_3$ and $EuSn_3$) and our results nice confirms this fact in both RIn_3 and RSn_3 cases. It is also reveals from the table that LDA and LDA+U underestimate the lattice parameter which is consistent with general trend of these approximations. Furthermore, the bulk moduli (Table I) are also calculated for the compounds under

TABLE I. The calculated value of lattice parameters (a in Å) and bulk modulus (B_0 in GPa) of RIn_3 and RSn_3 compounds.

Comp.		E_{xc}	a	B_o
$SmIn_3$	This work	LSDA	4.5645	60.4711
		GGA	4.6246	53.6537
		LDA+U	4.5595	56.2006
		GGA+U	4.7198	52.0019
	Expt.[a]		4.626	
$EuIn_3$	This work	LSDA	4.5707	63.7229
		GGA	4.6269	53.2488
		LDA+U	4.5639	63.2119
		GGA+U	4.7592	54.2521
$GdIn_3$	This work	LSDA	4.5167	62.3367
		GGA	4.5743	66.5797
		LDA+U	4.5075	66.2844
		GGA+U	4.6557	68.5292
	Expt.[a]		4.607	
$SmSn_3$	This work	LSDA	4.6052	68.8160
		GGA	4.6545	56.4352
		LDA+U	4.6135	65.4388
		GGA+U	4.7523	54.2082
	Expt.[b]		4.687	
$EuSn_3$	This work	LSDA	4.6313	73.2400
		GGA	4.6727	52.9966
		LDA+U	4.6316	58.2304
		GGA+U	4.7742	44.4547
	Expt.[b]		4.744	
$GdSn_3$	This work	LSDA	4.6412	61.0454
		GGA	4.6412	61.0453
		LDA+U	4.5947	72.2621
		GGA+U	4.7227	67.5417
	Expt.[b]		4.678	

[a]Ref. 47.
[b]Ref. 18.

investigation. So far we know, no experimental data are available for the bulk moduli and their pressure derivatives, so our result are considered as a prediction for these properties of RIn_3 and RSn_3 (R = Sm, Eu, and Gd).

IV. ELECTRONIC PROPERTIES

In order to understand the electronic properties of the compounds under investigation, we first incorporated the total DOSs and 4f DOSs with LDA and GGA. As in 4f orbital electron system, such as lanthanides the electronic correlation become so strong, so for better understanding the effect of 4f state, we adopt LDA+U, GGA+U, and spin orbit coupling is also involved. The total and 4f DOSs calculated with different exchange and correlation potentials for RIn_3 and RSn_3 (R = Sm, Eu, and GD) are shown in Figs. 1–3, respectively. The Fermi level is set at 0 eV. It is clear from the Figs. 1–3 that no band gaps are available at Fermi level for all these intermetallic compounds; hence all these compounds are metallic in nature. Fig. 1 presents the total DOS (blue lines) and 4f DOS (red lines) using GGA for these compounds. The dominating character around the Fermi level is from rare earth elements. The tail of 4f states also crosses the Fermi level except $GdIn_3$ and $GdSn_3$. For both $GdIn_3$ and $GdSn_3$, the 4f states lie below the Fermi level. From Fig. 1, we can see that the strong peaks which is due to 4f states located at −0.1 eV, −0.38 eV, −4.5 eV, −0.45 eV, −0.90 eV, and −4.5 eV for $SmIn_3$, $EuIn_3$, $GdIn_3$, $SmSn_3$, $EuSn_3$, and $GdSn_3$, respectively. In Fig. 2, we have reported the total and 4f DOSs within LDA+U (black lines) and GGA+U (red lines) schemes. It is clear from the figure that the maximum peaks which is due to 4f states are shifted towards lower energies as compared with GGA (Fig. 1), this is in agreement with previous DFT calculations that Hubbard U open the gap between occupied and unoccupied sates.[33] Fig. 3 shows the total and 4f DOSs with GGA+SO. One can see that the SOC does not change the energy position of 4f

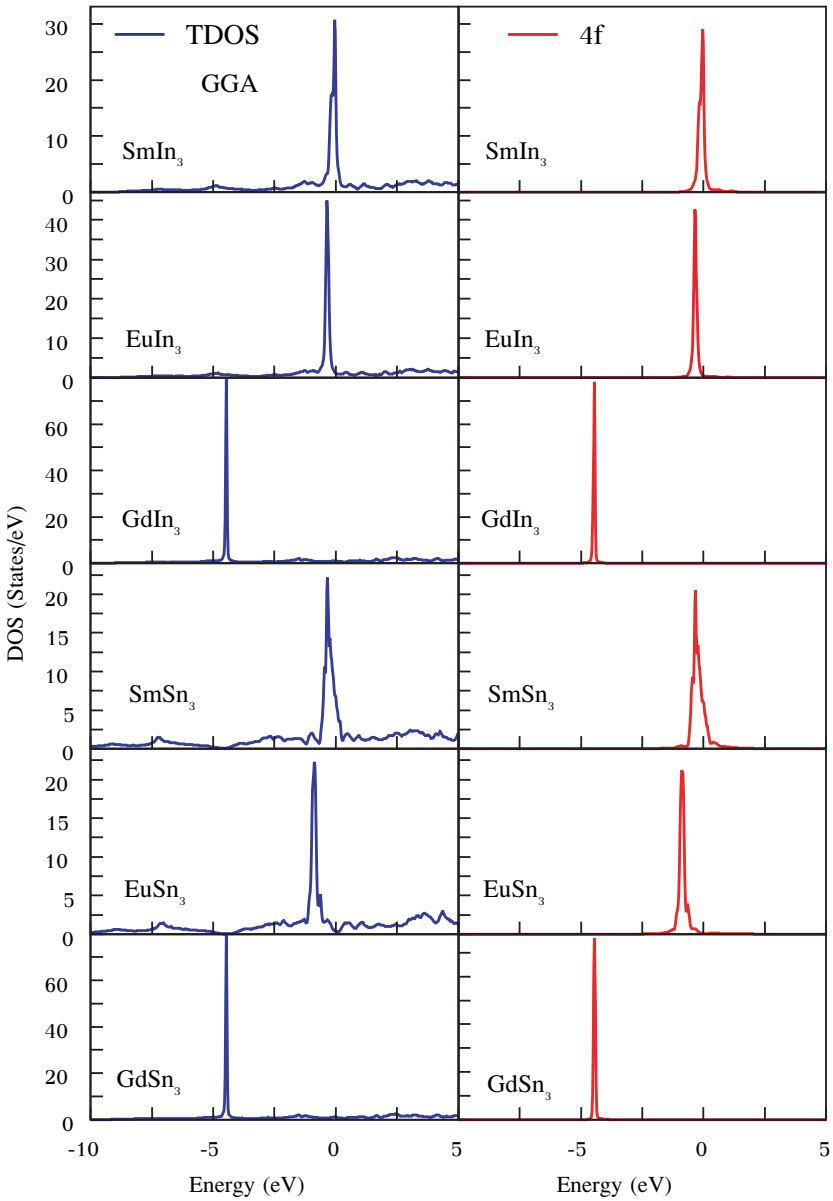

FIG. 1. Total density of states TDOS (blue lines) and partial 4f DOS (red lines) of RIn_3 and RSn_3 for R = Sm, Eu, and Gd calculated with GGA.

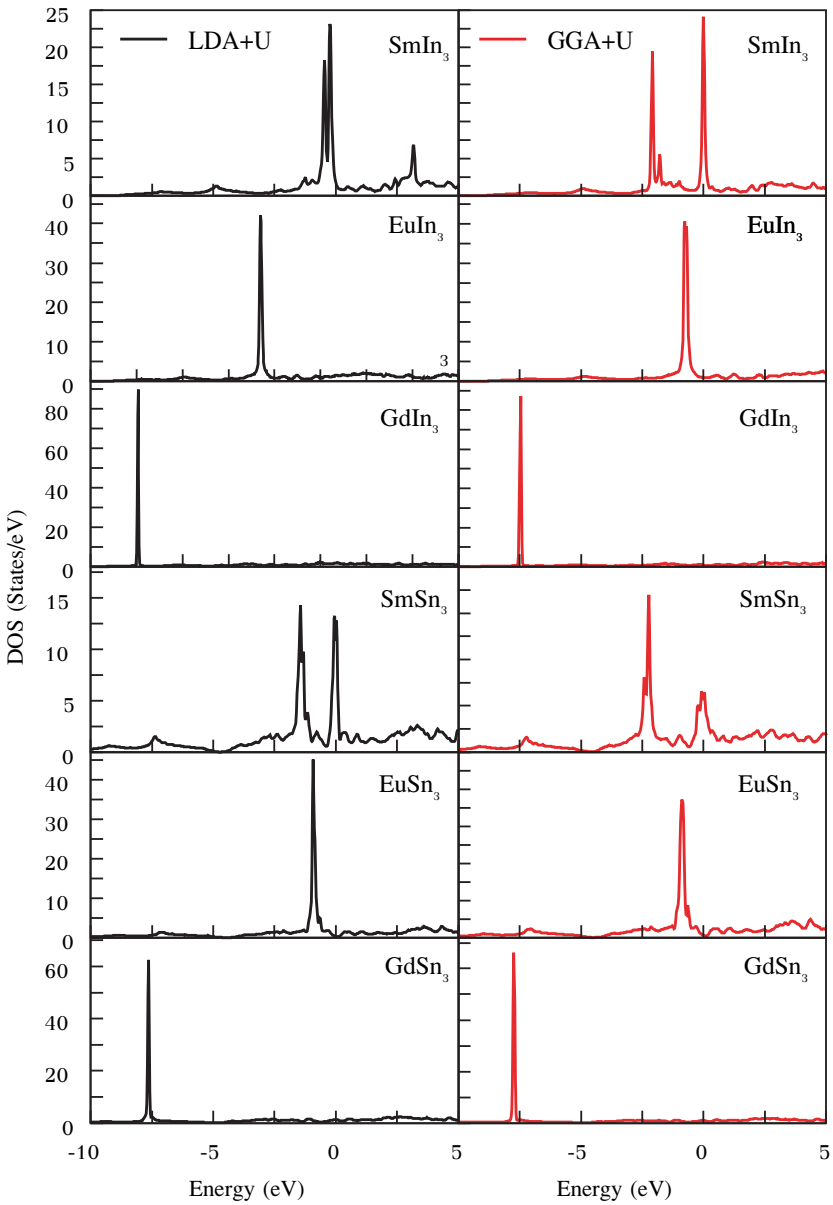

FIG. 2. Total density of states TDOS with LDA+U (black lines) and GGA+U (red lines) of RIn_3 and RSn_3 for R = Sm, Eu, and Gd.

states. SOC causes to remove the spin degeneracy and so 4f DOSs calculated by GGA, LDA+U and GGA+U are split into two peaks. The two peaks corresponding to j = 5/2 and j = 7/2. The peaks corresponding to j = 5/2 are filled in all compounds and the peaks corresponding to j = 7/2 are filled in $GdIn_3$ and $GdSn_3$ and partially filled in the remaining compounds. In RIn_3 and RSn_3 compounds the magnetic moment is arising from the f-electrons of lanthanides atom. The total DOSs for RIn_3 and RSn_3 (R = Sm, Eu, Gd) compounds in anti-ferromagnetic (AFM) phase are presented in Fig. 4. For AFM the calculations we construct $1 \times 1 \times 2$ cubic super-cell. It is clear from the figure that DOSs is symmetric in both spin up and spin down channels. Their magnetic moments are in opposite directions, which results in a zero total magnetic moment. At zero temperature all these compounds in question are in AFM phase. The calculated results are in good agreement with the experimentally[15–18] observed AFM-like behavior in RIn_3 and RSn_3 compounds at low temperature.

V. ELASTIC PROPERTIES

Elastic constants of a solid are very important that describe the response to the applied stress and especially they are related to different fundamental solid-state phenomena such as intra-atomic bonding, equations of state, phonon spectra, and structure stability. Elastic properties are also linked thermodynamically with specific heat, thermal expansion, Debye temperature, and Gruneisen parameter. The elastic properties of solids are the indicators of mechanical strength, which is a matter of great practical significance.

The three elastic constants C_{11}, C_{12}, and C_{44} for RIn_3 and RSn_3 (R = Sm, Eu, Gd) calculated with GGA approximation with and without spin polarization are listed in Table II. The only experimental available values of C_{11} and C_{44} for $SmIn_3$ and $SmSn_3$ (Ref. 21) have been compared. The experimental values of C_{11} and C_{44} are at 100 K and we have calculated the elastic constants at 0 K. Thus the different temperature causes the small disagreement between our calculated and

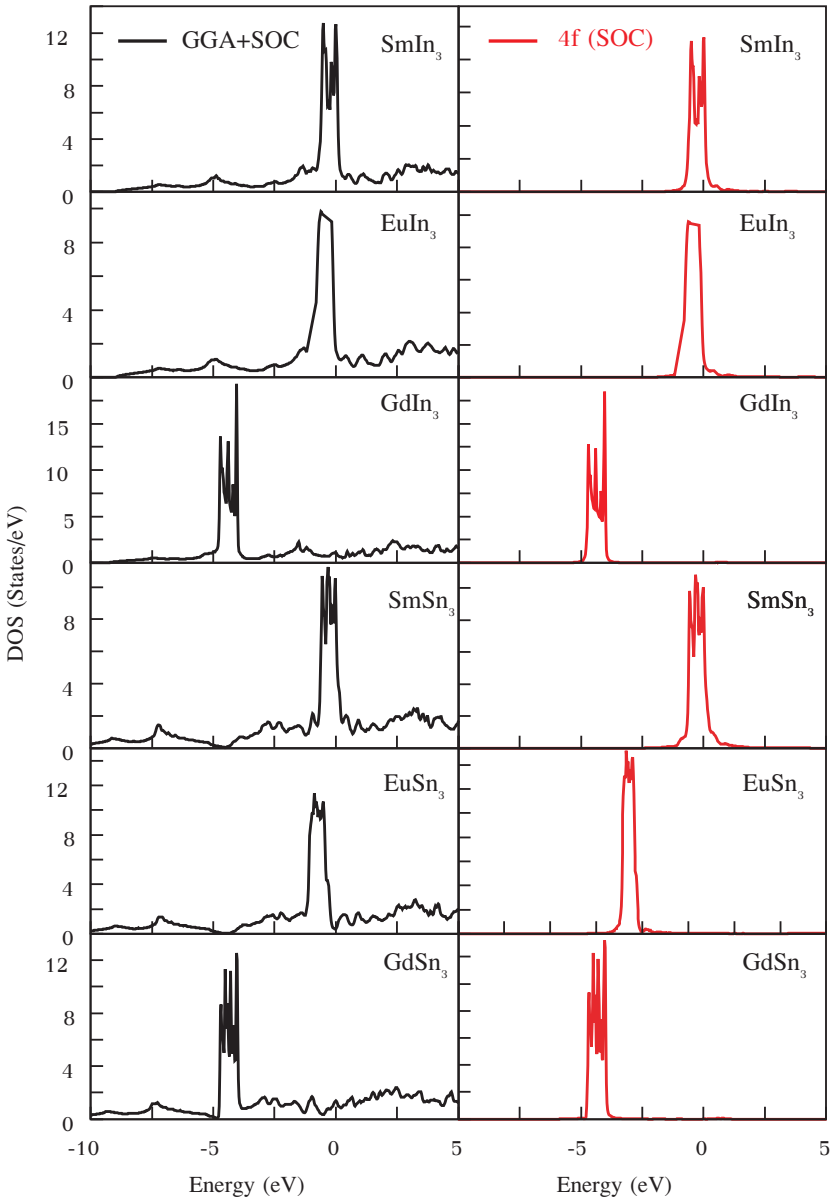

FIG. 3. Total density of states TDOS (black lines) of RIn_3 and RSn_3 and partail 4f DOS (red lines) for R = Sm, Eu, and Gd calculated with GGA+SOC.

experimental values. The stability of given crystal structure follow certain criteria. Furthermore, our calculated elastic constants fulfilled the required stability conditions for cubic structures, i.e., $C_{11}–C_{12}>0;\ C_{44}>0;\ C_{11}+2C_{12}>0$.[34,35] The fulfillment of the above criteria's justified that these intermetallic compounds are elastically stable.

Table II shows that the nonmagnetic phase largely influences the elastic properties of RIn_3 and RSn_3 compounds. Nonmagnetic ordering decreases the elastic constants value.

The mechanical parameters, such as bulk modulus B_0, shear modulus G, Young's modulus Y, Poisson's ratio ν, and anisotropic ratio A, which are the important elastic parameters for industrial applications, are calculated from the elastic constants C_{11}, C_{12}, and C_{44} of the compounds under investigation and reported in Table III. These are important parameters to characterize the mechanical behavior of a material. We explain the mechanical properties on the basis of results obtained by GGA spin polarized calculations.

The average shear modulus, $G = G_H$, is a measure resistance to plastic deformations upon shear stress.[36] As per Hill[37] average shear modulus, G is defined as arithmetic mean of Voigt shear modulus G_V and Reuss shear modulus G_R, which can be expressed in terms of elastic constants as

$$G_H = \frac{G_V + G_R}{2}, \tag{1}$$

where

$$G_v = \frac{1}{5}(3C_{44} + C_{11} - C_{12}), \tag{2}$$

$$G_R = \frac{5(C_{11} - C_{12})C_{44}}{4C_{44} + 3(C_{11} - C_{12})}. \tag{3}$$

The calculated value of G_H is given in Table III, which indicates that $GdSn_3$ exhibiting a largest value of G_H (44.082 GPa) and $GdIn_3$ is with lower value of shear modulus that is (27.962 GPa). The other compounds lie in the range between these two values.

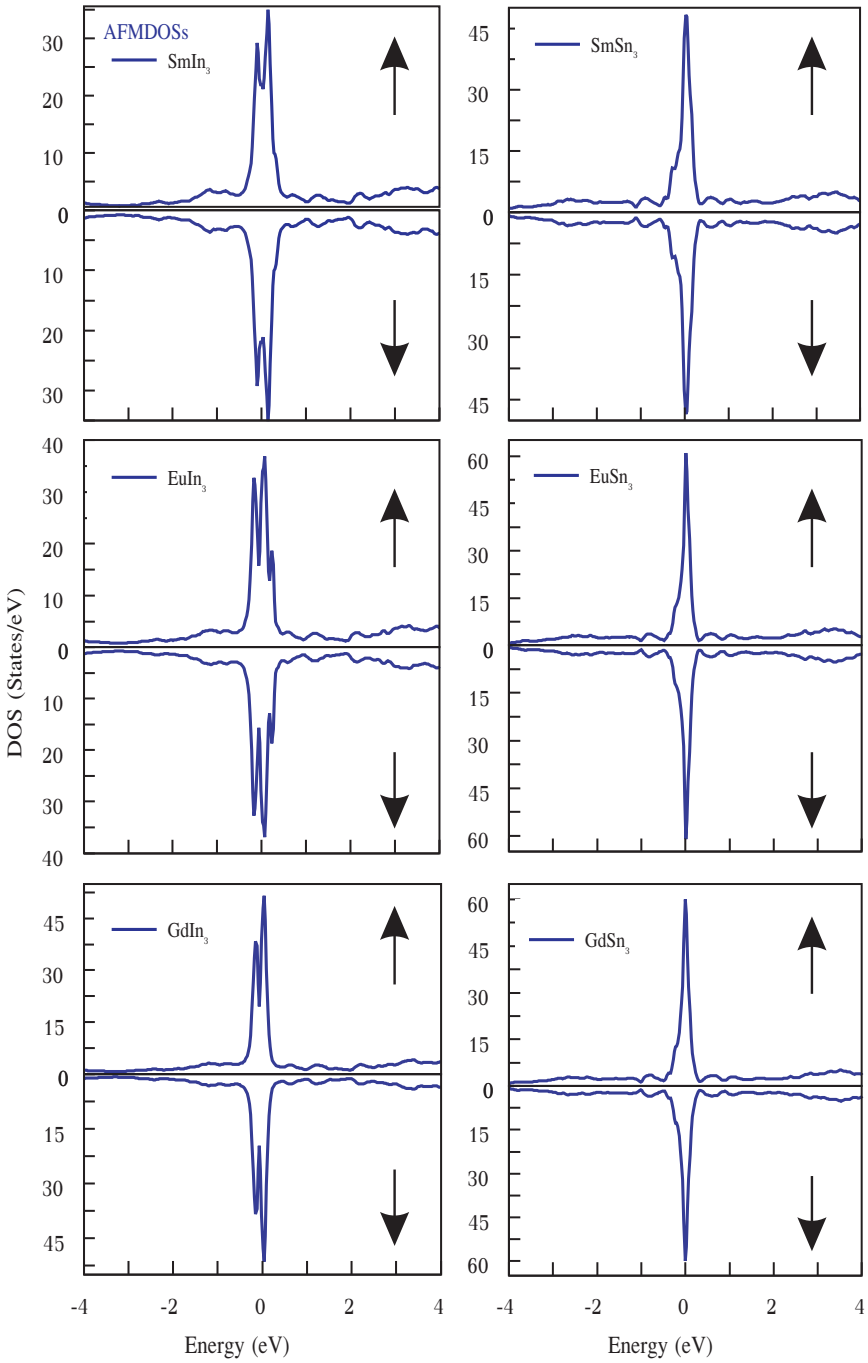

FIG. 4. AFM DOSs for the double cell of RIn_3 and RSn_3 for R = Sm, Eu, and Gd.

TABLE II. The calculated values of elastic constants C_{11}, C_{12}, C_{44} (GPa) with spin polarization (GGA+SP) and without spin polarization (GGA).

Comp.	E_{XC}	$SmIn_3$	$EuIn_3$	$GdIn_3$	$SmSn_3$	$EuSn_3$	$GdIn_3$
C_{11}	GGA+SP	139.068	113.716	119.369	93.191	118.316	128.143
	GGA	100.476	100.413	118.385	99.429	94.142	114.310
Exp.		125.3[a]			95.4[a]		
C_{12}	GGA+SP	60.276	56.308	63.034	42.836	61.175	59.806
	GGA	59.290	67.402	75.417	39.203	65.844	63.171
C_{44}	GGA+SP	28.171	28.450	27.862	43.003	51.377	52.275
	GGA	30.426	22.588	31.348	32.211	28.788	44.195
Exp.		32.9[a]			34.3[a]		

[a]Ref. 21.

The Young's modulus Y, the resistance of solid material to the linear strain along edges, defines as the ratio between stress and strain. The compound is stiffer for the larger value of Y. It can be find out from the computed values of Voigt shear modulus G_V and bulk modulus B_0 by following equation:

$$Y = \frac{9B_0G_V}{3B_0 + G_V}. \quad (4)$$

The presented valve of Young's modulus in Table III shows that $GdSn_3$ compound is stiffer than the other. Also the higher values of young modulus as compared to Bulk modulus these compounds indicted stiffness.

TABLE III. The calculated value of Voigt's shear modulus G_V, Reuss's shear modulus G_R, Hill's shear modulus G_H, B/G ratio, Cauchy Pressure (C''), Poisson's ratio (v), Kleinman Parameter (ξ), Anisotropy constant (A) Lames Coefficient (λ and μ), and Shear Constant (C').

Comp.	$SmIn_3$	$EuIn_3$	$GdIn_3$	$SmSn_3$	$EuSn_3$	$GdSn_3$
G_V	32.661	28.552	27.963	35.873	42.254	45.032
G_R	31.795	28.551	27.962	33.512	38.943	43.132
G_H	32.228	28.551	27.962	34.693	40.598	44.082
Y	87.034	76.060	75.308	89.640	107.831	114.318
B/G	2.685	2.642	2.926	1.719	1.976	1.873
C''	32.105	27.858	35.208	−0.167	9.798	7.531
ν	0.332	0.332	0.347	0.249	0.276	0.269
ξ	0.728	0.826	0.879	0.769	0.861	0.780
A	0.715	0.991	0.988	1.708	1.798	1.530
λ	64.766	56.410	63.171	35.706	52.052	52.563
μ	32.661	28.552	27.963	35.873	42.254	45.032
C'	39.396	28.704	28.168	25.178	28.571	34.169

The ductile/brittle behavior of the materials can be calculated by the ratio of bulk modulus to shear modulus (B/G) proposed by Pugh.[38] The critical value that separates the ductile and brittle character was found to be 1.75. A high B/G ratio is associated with ductility whereas a low value corresponds to a brittle nature of materials. It is clear from the Table III that all compounds shows ductile behavior, whereas $SmSn_3$ is brittle.

Cauchy's pressure is the difference between two particular elastic constant ($C'' = C_{12} - C_{44}$). Pittifor[39] suggest that Cauchy's pressure is used to describe the bonding character of the compounds under investigation. The positive value of Cauchy's pressure corresponds to metallic bonding while the materials with negative Cauchy's pressure attributed to the angular or directional bonding (covalent bonding). Increase in the negative value of Cauchy pressure leads to the more directional bonding, lower mobility characteristic of the material. Our calculated Cauchy's pressure for RIn_3 and RSn_3 (R = Sm, Eu, Gd) are given in the table predicted that all these compounds have positive Cauchy's pressure and thereby the metallic character in their bonds except $SmSn_3$ with negative value of Cauchy's pressure. The negative value of Cauchy's pressure for $SmSn_3$ indicated the directional or covalent bonding in this compound (brittleness).

Furthermore, the positive and negative values of Cauchy's pressure are the indicator of the ductile and brittle nature which confirms that $SmSn_3$, $EuIn_3$, $GdIn_3$, $EuSn_3$, and $GdSn_3$ are ductile whereas $SmSn_3$ is brittle.

The Poisson's ratio, ν, is calculated using the relation

$$\nu = \frac{3B_o - Y}{6B_o} = \frac{1}{2} - \frac{Y}{6B_o}. \quad (5)$$

Poisson's ratio is a measure of compressibility. As Poisson's ratio approaches to 0.5, the material have a tendency to incompressible;[40] and at $v = 0.5$, the material is near to incompressible. Our calculated values for v lie between 0.347 and 0.230, which indicate that these materials are less compressible and stable against elastic deformation. The v provides more information about the characteristics of the bonding forces. The lower limit and upper limit of Poisson's ratio v are given 0.25 and 0.5 for central forces in solids, respectively.[41] The calculated valves of v for the compounds under investigation show that the interatomic forces are central forces except $SmSn_3$ in which the interatomic central force is not predominant.

A parameter ζ introduced by Kleinman known as internal strain parameter.[42] It describes the relative tendency of bond bending versus the bond stretching. The lower limit ($\xi = 0$) corresponds to the minimizing bond bending term leads to and minimizing bond stretching term leads to upper limit ($\xi = 1$). Later, Harrison[43] linked the Kleinman parameter in an approximated way to the elastic constants by following equation:

$$\xi = \frac{C_{11} + 8C_{12}}{7C_{11} - 2C_{12}}. \quad (6)$$

Our calculated results of ζ range from ranging from 0.879 to 0.728 indicated that Bond bending is dominant in our materials. However, the lager value of ξ predicted that the contribution of bond stretching is also involved in these compounds.

The elastic anisotropic ratio A is another important parameter that determined whether the elastic properties or remain constant in different direction. Anisotropic ratio A is also closely related with the possibility of inducing microcracks into the materials and can be calculated from the following equation:[37]

$$A = \frac{2C_{44}}{C_{11} - C_{12}}. \quad (7)$$

A is unity for completely isotropic materials and the deviation from unity measures the amount of elastic anisotropy. The calculated values of anisotropic ratio A are given in Table III clearly indicated that these compounds are anisotropic.

Lame's constants (λ, μ) can be calculated from young modulus and Poisson's ratio by using following equation:

$$\lambda = \frac{Y\nu}{(1+\nu)(1-2\nu)}, \quad \text{and} \quad \mu = \frac{Y}{2(1+\nu)}. \quad (8)$$

Greater the value of young modulus greater will be the values of Lame's co-efficient. The two parameters together constitute a parameterization of the elastic moduli for homogeneous isotropic media. λ is known as Lame's first constant and μ is Lame's second constant. Their values for RIn_3 and RSn_3 (R = Sm, Eu, Gd) are given in Table III. Our results show that Lame's second modulus is equal to Voigt's shear modulus ($\mu = G_V$). For isotropic materials, $\lambda = C_{12}$ and $\mu = C'$. As our compounds are strongly anisotropic compounds and does not satisfied the condition for isotropic compounds, i.e., $\lambda = C_{12}$ and $\mu = C'$.

Another important parameter is the shear constant which has been calculated by using relation

$$C' = \frac{1}{2}(C_{11} - C_{12}). \quad (9)$$

Its values for the compounds under considerations are given in Table III. It is also known as tetragonal shear modulus. Dynamical stability require that $C' > 0$. The positive values of

TABLE IV. The calculated values of density ρ (g/cm^3), sound velocity of transverse wave v_s (m/s), sound velocity of longitudinal waves v_l (m/s), Debye average velocity v_m (m/s), and Debye temperature $\theta(D)$ (K) of compounds.

Comp.	ρ	v_l	v_s	v_m	$\theta(D)$
$SmIn_3$	7.813	4071.39	2030.98	2278.69	143.75
$EuIn_3$	7.652	3851.53	1931.63	2166.54	135.58
$GdIn_3$	8.254	3800.59	1841.57	2069.55	132.35
$SmSn_3$	7.835	3676.06	2104.25	2337.86	146.48
$EuSn_3$	7.553	4162.83	2288.30	2550.71	157.71
$GdSn_3$	8.092	4179.62	2334.02	2598.46	163.82

our calculated materials indicate that these are mechanically stable material. The bigger shear modulus corresponding the more rigidity the material to the tetragonal distortions.

We also calculated the thermo-physical properties like longitudinal v_l, transverse v_s, average v_m sound velocities, and Debye temperature $\theta(D)$ properties of these compounds.

The Debye temperature $\theta(D)$ can be calculated using the following classical relations:[44]

$$\theta(D) = \frac{h}{k_B}\left[\frac{3n}{4\pi}\left(\frac{N_A\rho}{M}\right)\right]^{\frac{1}{3}} v_m, \tag{10}$$

where h is the plank constant, K_B is the Boltzman constant, N_A is the avagadro number, ρ is the density, M is the molecular weight, v_m is the average sound velocity, and n is the number of atom per formula unit.

The average sound velocity in the polycrystalline material is approximately given by[45]

$$v_m = \left[\frac{1}{3}\left(\frac{2}{v_s^3} + \frac{1}{v_l^3}\right)\right]^{\frac{-1}{3}}, \tag{11}$$

where v_l and v_s are the longitudinal and transverse sound velocities, which can be obtained using the shear modulus G and the bulk modulus B_0 from Navier's equation, respectively,[46]

$$v_l = \left[\frac{B + \frac{4G}{3}}{\rho}\right]^{\frac{1}{2}}, \quad \text{and} \quad v_s = \left[\frac{G}{\rho}\right]^{\frac{1}{2}}. \tag{12}$$

The calculated values of the sound velocities, Debye temperature, as well as theoretical densities, which can be obtained from the elastic constants are presented in Table IV. It is clear from the Tables III and IV that the Debye temperature is directly related to the elastic moduli. Thus greater the elastic moduli, higher will be the Debye temperature. For the comparison, no experimental data are available in the literature. Future experimental work will verify these results. We consider the present results as a prediction study for these compounds with the hope that the future experimental work will test our calculated results.

VI. CONCLUSIONS

First principle calculations have been performed to theoretically studies the structural elastic, mechanical, and electronic properties of RIn_3 and RSn_3 (R = Sm, Eu, Gd) compounds using DFT. The ground state lattice parameters are in better agreement with the experiment. The electronic DOS shows the intermettalic nature of these compounds. The SOC further split 4f state into two states with changing the energy position of 4f states. The results show that these compounds are elastically stable and anisotropic. The higher values of young modulus indicated that these compounds are stiffer. The B/G ratio predicted that these compounds are ductile except $SmSn_3$. The sound velocities and Debye temperature are investigated for these compounds as the first time.

[1]T. Tsuchida and W. E. Wallace, J. Chem. Phys. **43**, 3811 (1965).
[2]K. H. J. Buschow, Ferromagnetic Mater. **1**, 297 (1980).
[3]K. A. Gschneidner, Jr., A. Russell, A. Pecharsky, J. Morris, Z. Zhang, T. Lograsso, D. Hsu, C. H. C. Lo, Y. Ye, A. Slager, and D. Kesse, Nature Mater. **2**, 587 (2003).
[4]K. A. Gschneidner, Jr., M. Ji, C. Z. Wang, K. M. Ho, A. M. Russell, Y. Mudryk, A. T. Becker, and J. L. Larson, Acta Mater. **57**, 5876 (2009).
[5]T. Iizuka, T. Mizuno, B. H. Min, Y. S. Kwon, and S. Kimura, J. Phys. Soc. Jpn. **81**, 043703 (2012).
[6]C. L. Lin, T. Yuen, and T. Mihalisin, Phys. Rev. B **54**, 9254 (1996).
[7]C. F. Li, Z. Q. Liu, P. J. Shang, and J. K. Shang, Scr. Mater. **65**, 1049 (2011).
[8]S. J. Asadabadi, S. Cottenier, H. Akbarzadeh, R. Saki, and M. Rots, Phys. Rev. B **66**, 195103 (2002).
[9]A. Bajorek, G. Chelkowska, A. Chrobak, and M. K. Grudziecka, Intermetallics **26**, 142 (2012).
[10]N. Nagai, I. Umehara, T. Ebihara, A. K. Albessard, H. Sugawara, T. Yamazaki, K. Satoh, and Y. Onuki, Physica B **186**, 139 (1993).
[11]Z. Kletowski, Solid State Commun. **72**, 901 (1989).
[12]K. H. J. Buschow, H. W. de Wijn, and A. M. van Diephen, J. Chem. Phys. **50**, 137 (1969).
[13]A. Percheron, O. Crorochov, and J. C. Achard, C. R. Acad. Sci. Paris C **277**, 81–83 (1973).
[14]R. Harris and G. V. Raynor, J. Less-Common Met. **9**, 7 (1965).
[15]K. H. J. Buschow, Phys. Lett. A **29**, 12 (1969).
[16]E. Gorlich, H. Hrynkiewicz, R. Kmied, K. Catka, K. Tomala, A. Czopnik, and N. Iliew, Phys. Status Solidi A **30**, K17 (1975).
[17]K. H. J. Buschow, Rep. Prog. Phys. **42**, 1373 (1979).
[18]J. P. Sanchez, J. M. Friedt, G. K. Shenoy, A. Percheron, and J. C. Achard, J. Phys. C: Solid State Phys. **9**, 2207 (1976).
[19]Y. Onuki and R. Settai, Low Temp. Phys. **38**, 89 (2012).
[20]S. J. Asadabadi and H. Akbarzadeh, Physica B **349**, 76 (2004).
[21]D. Endoh, T. Goto, A. Tamaki, B. Liu, M. Kasaya, T. Fujimura, and T. Kasuya, J. Phys. Soc. Jpn. **58**, 940 (1989).
[22]Z. Suna, S. Lib, R. Ahuja, and J. M. Schneidera, Solid State Commun. **129**, 589 (2004).
[23]P. Blaha, K. Schwarz, G. k. H. Madsen, D. Kuasnicka, and J. Luitz, *WIEN2K, An Augmented Plane Wave+Local Orbitals Program for Calculating Crystal Properties*, edited by K. Schwarz (Technical Universitat, Wien, Austria, 2001).
[24]O. K. Andersen, Phys. Rev. B **12**, 3060 (1975).
[25]J. P. Perdew and A. Zuanger, Phys. Rev. B **23**, 5048 (1981).
[26]J. P. Perdew, K. Burke, and M. Ernzerhop, Phys. Rev. Lett. **77**, 3865 (1996).
[27]V. I. Anisimov, I. V. Solovyev, M. A. Korotin, M. T. Czyzyk, and G. A. Sawatzky, Phys. Rev. B **48**, 16929 (1993).
[28]H. J. Monkhorst and J. D. Pack, Phys. Rev. B **13**, 5188 (1976).
[29]M. Jamal, Cubic-elastic, http://www.wien2k.at/reg_user/unsupported/ (2012).
[30]M. Jamal and S. Jalali Asadabadi, e-print arXiv:submit/0630082 [cond-mat.mtrl-sci] (2013).
[31]R. Stadler, W. Wolf, R. Podloucky, G. Kresse, J. Furthmuller, and J. Hafner, Phys. Rev. B **54**, 1729 (1996).
[32]F. Birch, Phys. Rev. **71**, 809 (1947).
[33]K. Tao, J. Zhou, Q. Sun, Q. Wang, V. S. Stepanyuk, and P. Jena, Phys. Rev. B **89**, 085103 (2014).
[34]M. Born and K. Huang, *Dynamical Theory of Crystal Lattices* (Clarendon, Oxford, 1954).
[35]J. Wang and S. Yip, Phys. Rev. Lett. **71**, 4182 (1993).
[36]W. Voigt, *Lehrbuch der Kristallphysik, Taubner, Leipzig* (1928).

[37]R. Hill, Proc. Phys. Soc. London **65**, 349 (1952).
[38]S. F. Pugh, Philos. Mag. **45**, 823 (1954).
[39]D. G. Pettifor, Mater. Sci. Technol. **8**, 345 (1992).
[40]P. H. Mott, J. R. Dorgan, and C. M. Roland, J. Sound Vib. **312**, 572 (2008).
[41]H. Fu, D. Li, F. Peng, T. Gao, and X. Cheng, Comput. Mater. Sci. **44**, 774 (2008).
[42]L. Kleinman, Phys. Rev. **128**, 2614 (1962).
[43]W. A. Harrison, *Electronic Structure and the Properties of Solids* (Freeman San Francisco, San Francisco, 1980).
[44]L. Fast, J. M. Wills, B. Johansson, and O. Eriksson, Phys. Rev. B **51**, 17431 (1995).
[45]O. L. Anderson, J. Phys. Chem. Solids **24**, 909 (1963).
[46]E. Schreiber, O. L. Anderson, and N. Soga, *Elastic Constants and their Measurements* (McGraw-Hill, New York, 1973).
[47]G. P. Schwartz and D. A. Shirley, Hyperfine Interact. **3**, 67 (1977).